

LOW-ENERGY ELECTRON DAMAGE OF DPPC MOLECULES - A NEXAFS STUDY*

R. Panajotović^{1**}, S. Ptasinska², V. Lyamayev³, and K. Prince⁴

¹University of Belgrade, Institute of Physics, Belgrade, Serbia

²University of Notre Dame, Department of Physics, South Bend, USA

³European XFEL GmbH, Hamburg, Germany

⁴Elettra Synchrotron Light Source, Trieste, Italy

Abstract. In cancer research the radiation dose delivered to different organs presents a critical parameter for destroying the cancer cells' DNA, but the biochemical pathways that bring cells to death in many cases start at the cell membrane whose major part consists of lipid molecules. In our XPS and NEXAFS experiment, we exposed a monolayer lipid film supported on gold to a spatially and energetically well defined electron beam (20 eV), simulating the charged particle avalanche produced in the exposure of the biological tissue to a high-energy ionizing radiation (X- and γ - rays, ions, etc). Oxygen and nitrogen 1s edge scans show a clear chemical degradation of the DPPC monolayer. The major damage has been inflicted to the polar head of the molecule and its links with the molecules' alkane chains.

Key words: DPPC, thin films, electron beam, NEXAFS, XPS.

DOI: 10.21175/RadJ.2016.01.09

1. INTRODUCTION

Phospholipids are amphiphilic molecules making a major part of the cell and organelle membrane. Their ordering, fluidity and orientation in solution and on various solid substrates, has been a subject of numerous biological study [1] because of the essential role it plays in the cell's survival; in chemical research [2, 3] for the variety of its structure and composition with other bio-active molecules; and in an extensive theoretical and experimental physics study [3, 4, 5] for their impressive property of a self-assembly as well as their permeability to charged particles and water. Experiments performed on mono- and bilayer films of phospholipids are often focused on the molecular orientation and packing in phase transitions at the air/water and air/solid interfaces, either as pure one-type layers or mixed phospholipid films [2, 3, 6]. The experimental techniques of the X-ray photoelectron spectroscopy (XPS) and Near-edge X-ray Absorption Fine Structure (NEXAFS), although performed under the non-biological conditions of the UHV, have given important answers about the structure and physico-chemical properties of such biomolecular targets [6-11]. The greatest advantage of these two techniques lies in the fact that they are very sensitive to the chemical changes at the very surface, but can also access the deeper lying parts of a bilayer, which is necessary for better understanding of the molecule-substrate interaction at the interface. Since in phospholipids the nitrogen and phosphorous atoms stoichiometric ratio is very small, the sensitivity of these two techniques is extremely useful in following the changes in chemical bonds in these atoms within the thin film.

1.1. DPPC

1,2-dipalmitoyl-sn-glycero-3-phosphocholine - DPPC (Figure 1) is a fully saturated phospholipid molecule widely used in the model-membrane and biomaterial studies [4, 10, 12]. It is suitable for production of artificial biomaterials and in combination with cholesterol and proteins presents a practical model for the study of transport and signalling in the model cell membrane. It is also a major component of the lung surfactant.

1.2. Low-energy electrons

Low-energy electrons ($E_0 < 30$ eV) are proved to be the most abundant secondary species created in the irradiation of the living tissue by high-energy ionizing

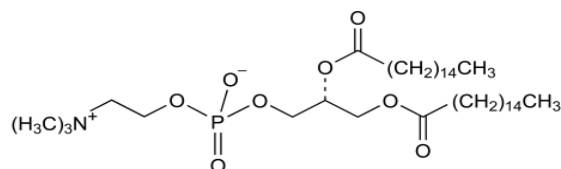


Figure 1. Chemical structure of DPPC. Polar head of the molecule consists of the negatively charged phosphate group and positively charged choline group. Two aliphatic tails are linked to the polar head via carboxylic groups.

radiation (X- and gamma- rays, ions, etc) [13]. They are responsible for the production of various molecular fragments from nucleic bases, and for breaking the strands of the DNA [13, 14, 15]. On the other hand, they also proved to be an efficient tool in the production of

* The paper was presented at the Third International Conference on Radiation and Applications in Various Fields of Research (RAD 2015), Budva, Montenegro, 2015.

** Contact: radmila@ipb.ac.rs

bio-chips on the SAM structure [5]. Therefore, a deeper insight into the interaction mechanisms between low-energy electrons and biomembrane molecules is necessary to understand the radiation effects and tailor the properties of the new bio-compatible materials and bioelectronic devices.

2. EXPERIMENT

NEXAFS and XPS measurements have been performed on the Material Science beamline (bending magnet) in Synchrotron light source installation - Elettra, Trieste, Italy. It provided the soft X-ray photon beam in the energy range from 22 to 1000 eV, mainly linearly polarized.

2.1. Preparation of thin lipid films

Samples were prepared on gold coated (30 nm) B-doped silicon wafer substrates bought from Georg Albert PVD Beschichtungen, Heidelberg, Germany. The substrates (polycrystalline Au (111), rms < 1 nm) have been cleaned in the Piranha solution (1:3 of 30% H₂O₂ and the 96% H₂SO₄ heated to 100 °C) and rinsed with copious amount of DI water. The monolayer of lipid molecules was formed in the Langmuir-Blodgett trough by dispensing sub-microliter drops of chloroform dissolved DPPC (16:0, from Avanti Polar Lipids, USA) on the clean surface of deionized water (R > 18 MΩ) and compressing to the surface pressure of 47 mN/m. This value corresponds to the surface pressure of the solid phase, i.e. closely packed and vertical molecules. Transfer of DPPC molecules to the solid substrate was done by pulling the gold substrates mounted on the holder through the stabilized DPPC/water interface. The pull-up speed of the gold substrate was 1 mm/min, which provided sufficient time for DPPC molecules to adhere to the substrate. The barriers of the LB trough were compressing the film to keep the surface pressure constant and below the value critical for the collapse of the monolayer (52 mN/m). This deposition procedure provided for the well-ordered lipid monolayer film with acyl-chains tilted at an angle corresponding to the ~ 30 mN/m [16] surface pressure at the water/air interface. The samples were let to dry in air before their mounting on the sample holder and introduction into the load-lock chamber, where they spent at least two hours in vacuum before the measurements were performed.

2.2. Experimental method

Electron irradiation has been performed with the existing LEED gun placed in the main vacuum chamber (analysis chamber) under the UHV ($p \sim 10^{-10}$ mb). Energy and beam size calibration of the gun was performed for two energies – 50 eV and 20 eV. As the electron beam at 20 eV was of a better shape and the size of the spot and the current on the sample allowed for gradual increase of the dose of electron irradiation of the monolayer film, we have used this energy to irradiate our samples. The dose of electron beam irradiation of the sample was comparable to the one used in our previous XPS measurements [17] (124 nA).

With this intensity and at the energy of 20 eV the LEED gun produced a collimated electron beam over the analysed sample area of 200 μm in diameter. We have performed two ten-minute electron-beam irradiations. Thus, the electron flux during one-time irradiation was ~ 2.4 mC/mm². If we take that the APM (Area-Per-Molecule) in the solid-supported film is ~48 Å² [16], then the electron beam delivered about 6700 electrons per molecule. The XPS data have been collected using the Al K_α monochromatic source with the energy of Al K_α 1486 eV and in the NEXAFS measurements we used synchrotron photon source with maximum energy of 1 keV. For the XPS measurement, the energy resolution of the analyzer was ~ 1 eV. Pass energy of the analyzer was 20 eV, angle of detection 20°, and the power of the source was 300 W. For the detailed spectra of carbon and oxygen bands, we performed ten scans, while for the nitrogen band, due to the inherent low ionization cross-section and low concentration (1/130 atoms in the DPPC

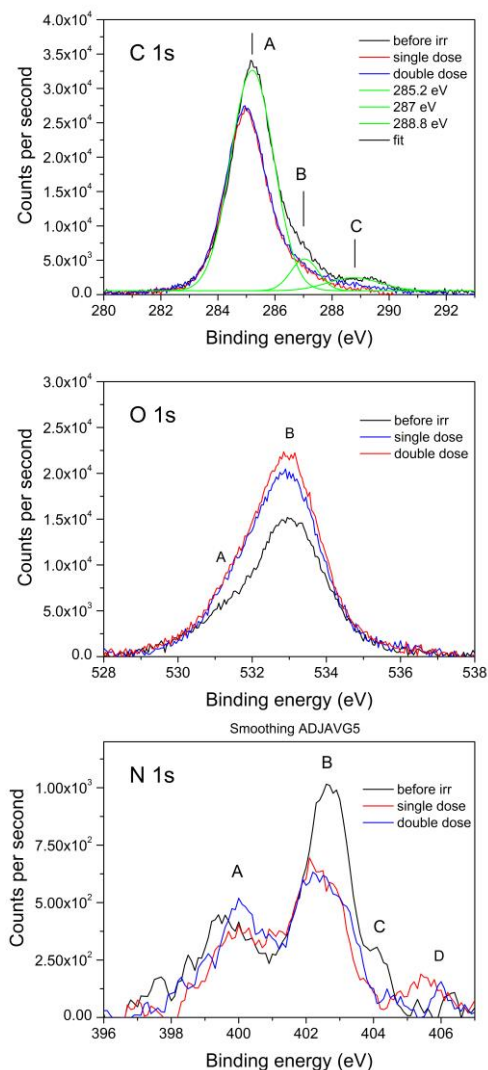


Figure 2. XPS scans of C 1s (a), O 1s (b) and N 1s (c) bands in DPPC before and after irradiation with 20 eV electrons. Low-level smoothing of the data has been applied to the N 1s curves for clearer view.

molecule), we collected photoelectrons over a five times longer time and at a half number of binding energy (BE) values.

NEXAFS measurements were performed for two angular orientations – normal and parallel incidence of the light beam, before and after electron irradiation. Since this technique probes the absorption of electromagnetic radiation (X-rays) by excitation of core electrons into unoccupied bound or continuum states, it allows access to a set of distinctive features (resonances) in the energy region from just below the absorption edge up to approximately 50 eV above the K-edge [8]. The position of the σ^* -resonances presents a measure of the intramolecular bond length while the π^* -resonances provide insight into bond hybridization [17].

2. RESULTS

In order to verify the existence of the material in the sample, including the level of its degradation after the irradiation with 20 eV-electron beam, we have performed the XPS measurements at the end station. The scans of the C 1s, O1s, and the N 1s bands in figure 2 clearly show the changes in the irradiated films, both in intensity of the secondary electron yield and the structure of peaks, i.e. binding energy. For all bond and resonance identifications we used the free database [19, 20] in addition to the reported data on nanomaterials [18] and standard organic molecules [6, 8-11, 21-25].

In the C 1s band, there are at least three peaks corresponding to BE of three functional groups in DPPC - 285.2 eV, 287 eV, and 288.8 eV. The main peak (A) corresponds to the aliphatic tails of the lipid molecule. It shifts to the lower binding energy corresponding to the native carbon (284.8 eV) and decreases in intensity after first irradiation, indicating the breakage of carbon bonds in the CH₂ chains. The other two (B and C) correspond to the overlapping of O-C=O and O-C-N bonds. It is evident from Figure 2 that the electrons induce chemical changes in the link of the two lipid tails (O 1s) and the choline group of the molecule (N 1s). As we were particularly looking at these two sites of bond damage, the next two band scans are of particular interest.

The O 1s band contains contribution from several bonds: C-O, C=O, P=O, P-O, and probably some contribution from bound water. Deconvolution of the oxygen spectrum is therefore very difficult. From studies of carbon nanomaterials [18, 2], we may interpret the shoulder in the region A at 531-532 eV as originating from C=O bonds, and the possible peak contribution in the region B from C-O at 533 eV. Close to this binding energy would be possible the contribution from bound water (~534 eV), and the one from phosphate group around 532 eV [9]. Although the

deconvolution of the O 1s structure is ambiguous, the effect of electron-irradiation is quite distinct. The region A clearly becomes more prominent and the oxygen peak gains both in width and intensity. This is likely due to the degradation of the C=O into the C-O bonds. An increase in the number of photoelectrons detected after electron-beam irradiation is not completely unexpected as the change in the bonds between the lipid head and acyl chains affects the orientation of the DPPC molecules in the monolayer. This would cause a decrease in attenuation of photoelectrons ejected from the O 1s state, which will increase the photoelectron yield.

The most complex effects of electron irradiation can be observed in the N 1s spectral band. The four regions in the spectrum show significant chemical changes in the DPPC films. In the A region the shift in energy after electron impact is from 399.5 eV to 400 eV, followed by the slight increase and then decrease in intensity. In the region B (402.6 eV) the shift is smaller (~ 200 meV) towards the lower binding energy and the intensity is decreased by 35 % after electron irradiation. In the region C (404 eV), the shoulder completely disappeared and in the region D (406.3 eV) the feature gradually shifted to the lower BE (405.5 eV) and increased in intensity. The region A corresponds to nitrogen in organic matrix in the cyanide type bond C-N- (~ 399.4 – 400.6 eV). The most affected region B corresponds to the N-(CH₃)₃ group overlapping with nitrite and nitrate compounds, as well as ammonium phosphate arising from the intermolecular bonding in the monolayer lipid film. The possible existence of nitro groups further indicates the increased complexity of the O 1s structure.

From the NEXAFS scan at the O 1s edge, taken for the grazing and normal incidence of the light, it is evident that the major change in oxygen bonds is taking place in σ^* resonances. In grazing incidence (GI), the decrease in the π^* resonance (π orbitals normal to the surface absorb the most light) takes place, and the shift in its energy is from 533 to 532.6 eV. At the same time, the σ^* resonance (region B and C) does not change much, indicating that the σ bonds in the sample oriented parallel to the surface are not significantly affected by the electron beam. For the normal incidence (NI) of light (maximum absorption for σ bonds perpendicular to the surface and π bonds lying on the surface), B-C region is narrower than in the grazing incidence scan. As in the XPS spectrum, because of the variety of bonds in the DPPC sample including oxygen, it is not quite clear which bonds are oriented in which direction. However, the NI scan reveals a remarkable degradation in σ bonds of DPPC molecules. Instead of one broad resonance, electron beam carves two distinct features at 537.8 eV and 540.2 eV, with the third making a shoulder at 542.6 eV.

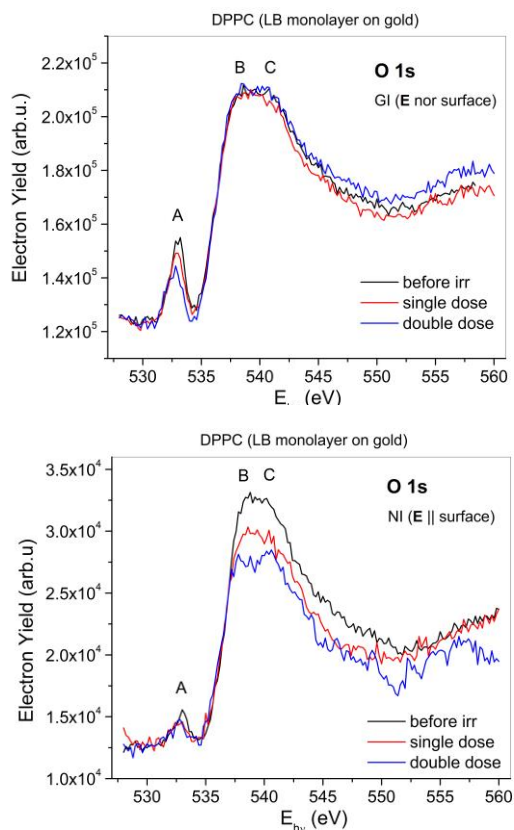


Figure 3. NEXAFS measurement at the O 1s edge – (a) grazing incidence and (b) normal incidence of the photon beam.

Grazing incidence scan (Figure 4) at the N 1s edge (the statistics in NI signal was too low) also features four distinct regions. The π^* resonance at 402.2 eV stays the same as before irradiation, but the new feature appears at 400.6 eV after the second irradiation, which may indicate the decomposition of

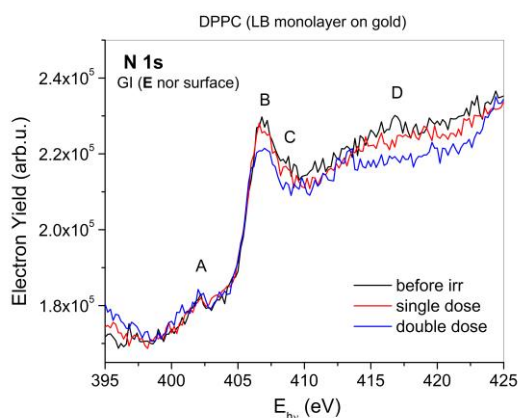


Figure 4: NEXAFS at the N 1s edge – normal incidence of photon beam.

C-N bonds in N-(CH₃)₃. In the σ^* resonance region, on the other hand, a relatively broad feature (406.6 – 407.4 eV) only diminishes in height, but the distinct separation in energy of different bonds is not achieved.

However, the shoulder in region C, at the energy of 408.6 eV completely disappears, as is the case with the resonance in the region D at 416.8 eV. There is also a possibility of the creation of the new nitrate or ammonium feature at 413 eV, but the insufficient statistics does not allow us to claim this with certainty.

3. CONCLUSION

The problem of radiation damage in the cell and organelle membrane is particularly important considering the complexity of its role in cell's metabolism. The integrity and stability of the lipid matrix making the major part of the bio-membrane is not only compromised by the direct absorption of high-energy ionizing radiation, but also by the effects of collisions from slow secondary electrons produced from ionization of the biological medium. For the purpose of better understanding the physicochemical mechanism behind the electron-lipid molecule interactions, a monolayer of DPPC molecules supported on gold substrate has been exposed to the monoenergetic electron beam and the bond damage analyzed by means of the X-ray photoelectron and near-edge X-ray fine structure. We have demonstrated that the electrons of 20 eV have capacity to induce significant damage to the lipid structure, and even incite the creation of new chemical groups. In particular, the bond cleavage of the carboxylic bonds linking two lipid tails to their polar head, and the degradation of the choline group of the molecule, point to the detrimental effect those secondary electrons from radiation may have on the conformation and functioning of lipids. This damage may be even enhanced in physiological conditions, where phase transitions from lamellar to non-lamellar form may induce a leaky structure incapable of maintaining the necessary boundary for the cell. Therefore, further study of the effects of low-energy charged particle /cell membrane interaction, on a model membrane, or in physiological conditions would be highly desirable.

Acknowledgement: The research presented in this paper was partially funded by the MCIRG-2007 research grant and the project OI171005, funded by the Ministry of Education, science and technological development of the Republic of Serbia. R. P. would like to thank the colleagues of the SAXS beamline at Elettra for the use of their chemical laboratory.

REFERENCES

1. T.A. Legace and N.D. Ridgway, "The Role of Phospholipids in the Biological Activity and the Structure of the Endoplasmic Reticulum," *BBA – Molec. Cell Res.*, vol. 1833, no. 11, pp. 2499-2510, Nov. 2013.
2. S. Mukherjee and A. Chattopadhyay, "Influence of Ester and Ether Linkage in Phospholipids on the Environment and Dynamics of the Membrane Interface: A Wavelength-Selective Fluorescence Approach," *Langmuir*, vol. 21, no. 1, pp. 287-293, Nov. 2005.

3. R.A. Bckmann and H. Grubmuller, "Multistep Binding of Divalent Cations to Phospholipid Bilayers: A Molecular Dynamics Study," *Angew. Chem. Int. Ed.*, vol. 3, no. 8, pp. 1021–1024, Feb. 2004.
4. E.T. Castellana and P.S. Cremer, "Solid Supported Lipid Bilayers: From Biophysical Studies to Sensor Design," *Surface Sci. Rep.*, vol. 61, no. 10, pp. 429–444, 2006.
5. A. Turchanin et al., "Molecular Self-Assembly, Chemical Lithography, and Biochemical Tweezers: A Path for the Fabrication of Functional Nanometer-Scale Protein Arrays," *Adv. Mat.*, vol. 20, no. 3, pp. 471-477, Feb. 2008.
6. G. Ketteler et al., "In Situ Photoelectron Spectroscopy Study of Water Adsorption on Model Biomaterial Surfaces," *J. Phys. Condens. Matt.*, vol. 20, no. 18, pp. 184024, Apr. 2008.
7. X. Liu et al., "Self-Assembly of Biomolecules at Surfaces Characterized by NEXAFS," *Can. J. Chem.*, vol. 85, no. 10, pp. 793-800, 2007.
8. G. Hähner, "Near Edge X-Ray Absorption Fine Structure Spectroscopy as a Tool to Probe Electronic and Structural Properties of Thin Organic Films and Liquids," *Chem. Soc. Rev.*, vol. 35, no. 12, pp. 1244-1255, Dec. 2006.
9. N.T. Samuel, C.Y. Lee, L.J. Gamble, D.A. Fischer and D.G. Castner, "NEXAFS Characterization of DNA Components and Molecular-Orientation of Surface-Bound DNA Oligomers," *J. Elect. Spec. Rel. Phen.*, vol. 152, no. 3, pp. 134-142, July 2006.
10. V. Cherezov, K.M. Riedl and M. Caffrey, "Too Hot to Handle? Synchrotron X-Ray Damage of Lipid Membranes and Mesophases," *J. Synchr. Rad.*, vol. 9, no. 6, pp. 333-341, Nov. 2002.
11. E. Novakova, G. Mitrea, C. Peth, J. Thieme, K. Mann, and T. Salditt, "Solid Supported Multicomponent Lipid Membranes Studied by X-Ray Spectromicroscopy," *Biointerph.*, vol. 3, no. 2, pp. FB44-FB54, June 2008.
12. LIPID Metabolites and Pathways Strategy "Lipid MAPS", Data bases. Retrieved from: <http://www.lipidmaps.org/resources/services.html>.
13. L. Sanche, "Low Energy Electron-Driven Damage in Biomolecules," *Eur. Phys. J. D*, vol. 35, no. 2, pp. 367-390, Aug. 2005.
14. R. Panajotovic, F. Martin, P. Cloutier, D. Hunting and L. Sanche, "Effective Cross Sections for Production of Single-Strand Breaks in Plasmid DNA by 0.1 to 4.7 eV Electrons," *Rad. Res.*, vol. 165, no. 4, pp. 452-459, Apr. 2006.
15. R. Panajotovic, M. Michaud and L. Sanche, "Cross Sections For Low-Energy Electron Scattering From Adenine in the Condensed Phase," *Phys. Chem. Chem. Phys.*, vol. 9, no. 1, pp. 138-148, Jan. 2007.
16. E.B. Watkins, C.E. Miller, W.P. Liao, and T.L. Kuh, "Equilibrium or Quenched: Fundamental Differences between Lipid Monolayers, Supported Bilayers, and Membranes," *ACS Nano*, vol. 8, no. 4, pp. 3181-3191, 2014.
17. R. Panajotovic, M. Schnietz, A. Turchanin, N. Mason, N. Mason, and A. Golzhauser, "Degradation of Phospholipid Molecules by Low-Energy Electrons," *Book of Abstr. Rad. Res. Soc. Conf.*, Sep. 25-29, 2010, Maui (Hi), USA, p.99.
18. T. Hemraj-Benny et al., "Near-Edge X-ray Absorption Fine Structure Spectroscopy as a Tool for Investigating Nanomaterials," *Small*, vol. 2, no. 1, 26-35, 2006.
19. Community site for x-ray absorption fine-structure "XAFS". Retrieved from: <http://www.xafs.org>.
20. A.V. Naumkin, A. Kraut-Vass, S.W. Gaarenstroom and C. J. Powell, Eds., "NIST X-ray Photoelectron Spectroscopy Database," Measurement Services Division of the NIST, USA, ref. db. 20, ver. 4.1, 2012. Retrieved from: <http://srdata.nist.gov/xps/>
21. T.K. Sham, B.X. Yang, J. Kirz, J.S. Tse, "K-edge Near-Edge X-Ray-Absorption Fine Structure of Oxygen- and Carbon-Containing Molecules in the Gas Phase," *Phys. Rev. A*, vol. 40, no.2, pp. 652-669, Aug. 1989.
22. S. Bhattacharayya, M. Lubbe, P.R. Bressler, D.R. T. Zahn, F. Richter, "Structure of Nitrogenated Amorphous Carbon Films from NEXAFS", *Diamond and Rel. Mat.*, vol. 11, no. 1, pp. 8-15, Jan. 2002.
23. P. Leinweber et al., "Nitrogen K-Edge XANES – an Overview of Reference Compounds Used to Identify 'Unknown' Organic Nitrogen in Environmental Samples," *J. Synch. Rad.*, vol. 14, no. 6, pp. 500-511, Nov. 2007.
24. S.S. Roy, P. Papakonstantinou, T.I.T. Okpalugo, and H. Murphy, "Temperature Dependent Evolution of The Local Electronic Structure of Atmospheric Plasma Treated Carbon Nanotubes: Near Edge X-Ray Absorption Fine Structure Study," *J. Appl. Phys.*, vol. 100, no. 5, pp. 053703, Sep. 2006.
25. L. Pasquali et al., "UPS, XPS, and NEXAFS Study of Self-Assembly of Standing 1,4-Benzenedimethanethiol SAMs on Gold," *Langmuir*, vol. 27, no. 8, pp. 4713–4720, Mar. 2011.